Available online at www.sciencedirect.com
ScienceDirect
Thin Solid Films 516 (2008) 3741 – 3746
thin solid films
www.elsevier.com/locate/tsf

Preparation and characterization of atomically flat and ordered silica films on a Pd(100) surface

Zhen Zhang, Zhiquan Jiang, Yunxi Yao, Dali Tan, Qiang Fu, Xinhe Bao *

State Key Laboratory of Catalysis, Dalian Institute of Chemical Physics, the Chinese Academy of Sciences, Dalian 116023, PR China

Received 8 November 2006; received in revised form 4 June 2007; accepted 7 June 2007
Available online 15 June 2007

Abstract

Ultrathin silica films with different thicknesses have been grown on a Pd(100) surface by depositing silicon in the presence of O_2. The film composition and electronic properties were characterized by X-ray photoelectron spectroscopy (XPS), ultraviolet photoelectron spectroscopy (UPS), and high-resolution electron energy loss spectroscopy (HREELS). Scanning tunneling microscopy was applied to investigate the film morphology and lattice structure. The results show that the obtained films are atomically flat and highly ordered in a long range. UPS and HREELS measurements indicate that the silica film has the same electronic and vibrational properties as bulk silica. A 2.8 nm thick film exhibits low defects in the film and high thermal stability up to 800 K, as evidenced by ion scattering spectroscopy and XPS.
© 2007 Elsevier B.V. All rights reserved.

Keywords: Silica films; Metal-oxide interfaces; X-ray photoelectron spectroscopy; Ultraviolet photoelectron spectroscopy; High-resolution electron energy loss spectroscopy; Scanning tunneling microscopy

1. Introduction

Silicon dioxide (SiO_2) is extensively used as a catalyst support. For surface scientists it is highly desirable to develop model catalysts consisting of metal clusters or nanoparticles supported on the surfaces of SiO_2. However, the insulating properties of bulk silica cause many experimental difficulties, such as surface charging, sample mounting, sample heating and cooling.

In order to circumvent these difficulties and to explore microprocesses on a silica surface (such as nanoparticle growth, surface chemical reaction, and thus induced structure change, etc. [1–6]) using surface analysis techniques, several methods have been recently developed to synthesize ultrathin SiO_2 films, among which two methods are frequently used. One is to directly expose single crystal silicon surfaces to oxygen, as in the case of Si(111)-7×7 [1–3] and Si(100) [4,5]; the other is to deposit silicon in an oxygen atmosphere or to oxidize a silicon layer on a metal substrate, such as Mo(110) [6–8], Mo(100) [9], Mo(112) [10–14], and Ni(111) [15]. Numerous studies have been performed on the preparation and characterization of thin SiO_2 films; while a few works are on the growth of ordered SiO_2 films. Freund's group and Goodman's group have prepared monolayer crystalline silica films on Mo(112) surfaces. The typical recipe for the growth of SiO_2 on Mo(112) consisted of repeated cycles of depositing one-half monolayer of silicon onto a Mo(112) surface at room temperature (RT) followed by oxidation at 800 K. The resulting SiO_2 films were subsequently annealed in four steps, which took 15 min each in an O_2 background of 1×10^{-3} Pa with the temperature ranging from 1100 to 1250 K [12,13]. Kundu and Murata reported growth of a 4.0 nm thick crystalline SiO_2 film on a Ni(111) surface [15]. Si was deposited on a clean Ni(111) surface at RT with 3 nm thickness followed by oxidation in the presence of atomic hydrogen for 1 h at a substrate temperature of 620 K. Finally the sample was annealed at 1100 K in an ambient O_2 atmosphere of 2.6×10^{-5} Pa for 10 min.

In this paper, we report a system for easily growing atomically flat and well-ordered silica films. In our growing system, Pd(100) was chosen as a substrate, and silica films were

* Corresponding author. Tel.: +86 411 84686637; fax: +86 411 84694447.
E-mail address: xhbao@dicp.ac.cn (X. Bao).

0040-6090/$ - see front matter © 2007 Elsevier B.V. All rights reserved.
doi:10.1016/j.tsf.2007.06.070

grown by depositing silicon onto Pd(100) in the presence of O_2. The morphologies, electronic properties, and thermal stabilities of films have been investigated by scanning tunneling microscopy (STM), X-ray photoelectron spectroscopy (XPS), ultraviolet photoelectron spectroscopy (UPS), high-resolution electron energy loss spectroscopy (HREELS), and ion scattering spectroscopy (ISS).

2. Experimental details

The experiments were carried out in an Omicron multiprobe surface analysis system with a base pressure of below 3.0×10^{-8} Pa. The system consists of three ultrahigh vacuum chambers: preparation, spectroscopic and microscopic chambers. The preparation chamber is equipped with a silicon evaporator and an ion-sputtering gun for sample cleaning. The spectroscopic chamber is installed with XPS, UPS, ISS, and HREELS (LK-ELS5000). The microscopic chamber is equipped with STM (Omicron Variable-Temperature STM). The three chambers are connected with a transfer chamber, through which the sample can be transferred among these chambers by magnetically coupled probes without breaking the vacuum.

A Pd(100) single crystal was mounted on an Omicron sample plate and can be resistively heated by a pyrolytic boron nitride heater. A chromel–alumel thermocouple was spot-welded on the back side of the Pd crystal to monitor the substrate temperature. The Pd(100) sample was cleaned by repeated Ar^+ sputtering, annealing, and oxidation treatment (in $\sim10^{-4}$ Pa O_2 at >700 K) in the preparation chamber until no contaminants were detected by UPS and XPS [16, 17]. The silicon evaporator was made of a silicon strip ($\sim1\times3\times10$ mm^3), which was cut off from a high purity silicon wafer and heated by running current through the strip. Silicon dioxide is formed on the substrate at 500 K when silicon is evaporated in a 1×10^{-3} Pa O_2 background atmosphere. After the deposition of the silica films, the heating power was turned off and the oxygen pressure was still maintained for another 5 min.

The XPS data were acquired with Mg Kα ($h\nu=1253.6$ eV) radiation and the spectra were calibrated with the Pd $3d_{5/2}$ peak at 335.1 eV [18]. The pass energy of the spectrometer was 30 eV, and the Pd $3d_{5/2}$ peak exhibited a full width at half maximum (FWHM) of 1.4 eV. All UP spectra were recorded at normal emission and the photoelectron peak positions were measured with respect to the Pd(100) Fermi level (E_F). ISS spectra were collected with an incident He^+ beam energy of 1000 eV. The energy resolutions of the HREELS measurements were between 40 and 64 cm^{-1} (5–8 meV). The monochromatized electrons were incident at an angle of 55° with respect to the surface normal of the sample. The analyzer could be rotated about its axis for in- and/or off-specular measurements. The

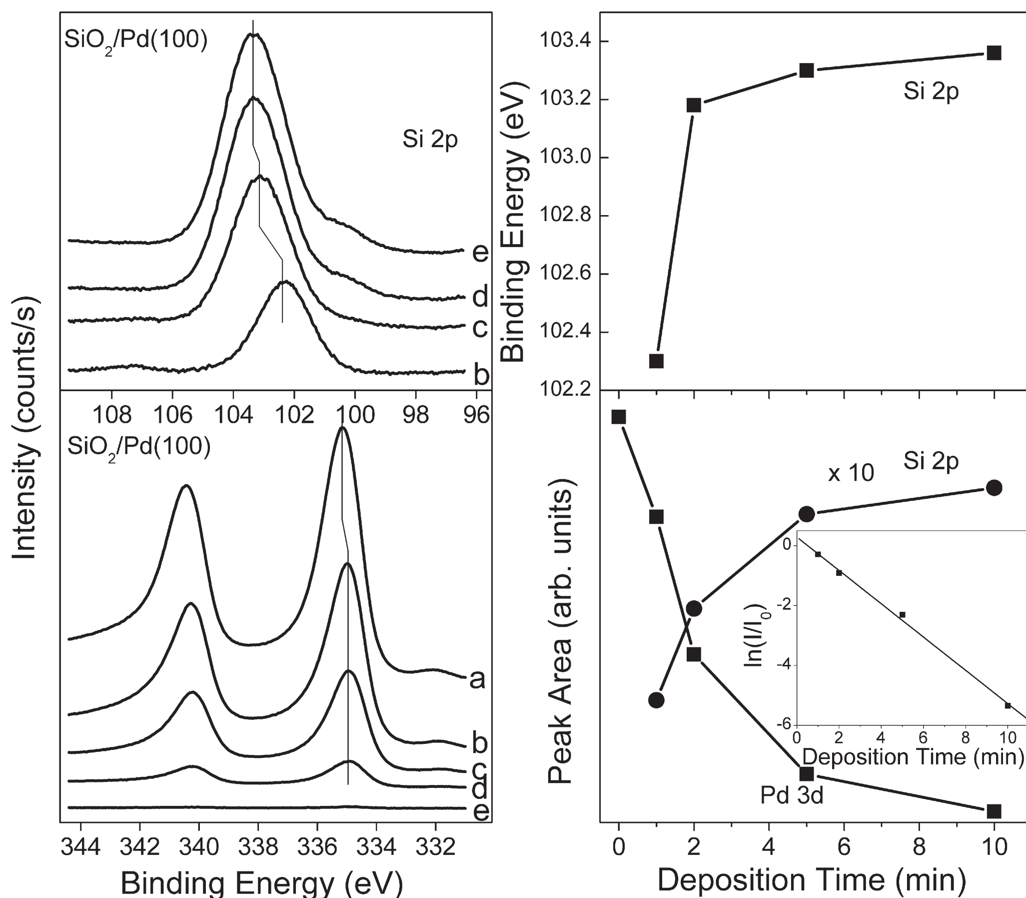

Fig. 1. Left: Si 2p and Pd 3d XP spectra of silica films on a Pd(100) surface with different thicknesses: (a) bare Pd(100), (b) 0.4 nm, (c) 1.1 nm, (d) 2.8 nm, (e) 6.5 nm; Right: (Upper) Si 2p binding energy as a function of deposition time; (Lower) Pd 3d and Si 2p peak areas as a function of deposition time; (Lower inset) Semi-logarithmic plot of the Pd 3d (signal normalized to the bare Pd(100) without SiO_2 deposition) versus deposition time.

primary energy (E_p) was 7.2 eV. An Omicron STM measurement was carried out at RT with a constant current mode using a homemade W-tip.

3. Results and discussion

The thickness of silica films was controlled by the deposition time of Si in O_2. A simple inelastic attenuation model was applied to estimate the film thickness, d, using the relation of

$$d = rt = -\lambda \cos\alpha \ln(I/I_0). \tag{1}$$

t is the deposition time of Si in O_2, r is the growth rate, I_0 and I are the XPS intensity of Pd 3d core level from bare Pd(100) and Pd(100) after deposition of SiO_2, α (63°) is the take-off angle with respect to the surface normal, λ is the electron inelastic mean free path. In our work, λ for Pd 3d peak with kinetic energy of 918.5 eV is taken as 26.9 Å, calculated according to Eq. (2) [19],

$$\lambda(\text{Å}) = \mathrm{k}[\mathrm{E(eV)}]^{\mathrm{p}} \tag{2}$$

where k and p corresponding to SiO_2 are 0.218 and 0.706 respectively.

Pd 3d and Si 2p spectra at different coverage of silica films are shown in Fig. 1. The integrated peak areas of the Pd 3d and Si 2p are plotted as a function of deposition time. The linear fit of the semi-logarithmic plot of I(Pd 3d)/I_0(Pd 3d) versus deposition time indicates a growth rate, r, of ~6 Å/min. The calculated silica film thicknesses are 0.4, 1.1, 2.8 and 6.5 nm corresponding to different deposition time 1, 2, 5 and 10 min, respectively. The similar method has been used to estimate the thickness of MgO and SiO_2 thin films grown on Mo substrates [7,20].

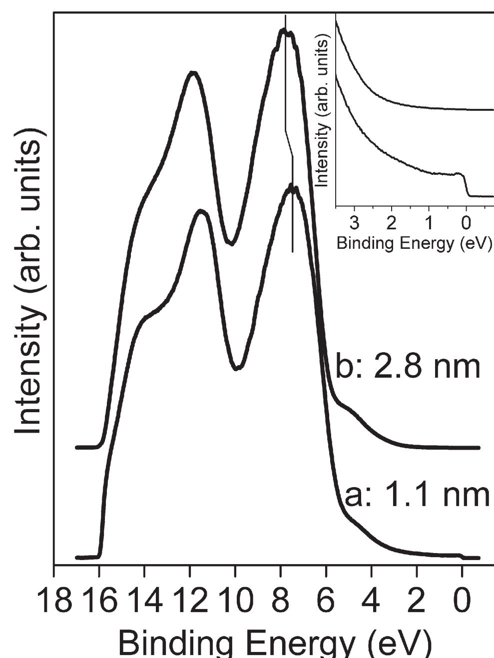

Fig. 2. Valence band data excited with He I (hν=21.2 eV) radiation from silica films with the thickness of (a) 1.1 nm and (b) 2.8 nm. Magnified spectra near E_F are shown in the inset.

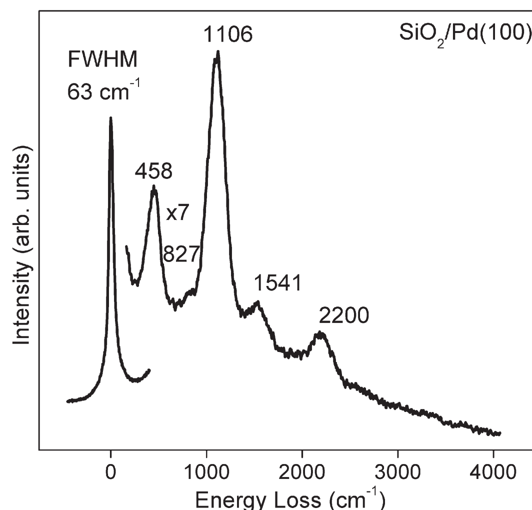

Fig. 3. HREEL spectra of SiO_2 film with 2.8 nm thickness.

Fig. 1 also shows that the Si 2p peak shifts to higher binding energy with an increase of the film thickness. For the 0.4 nm film, the Si 2p peak is located at 102.3 eV. The Si 2p peak shifts to 103.2 eV at the film thickness of 1.1 nm. Further increase of the thickness does not induce any obvious shift of the peak, as shown in the right panel, and finally the peak position reaches to 103.4 eV in the case of 6.5 nm film. This peak position is close to that of bulk SiO_2, which is at 103.3 eV [18]. The main peaks of the Si 2p spectra can be fitted by one component with FWHM around 2.3 eV. The result indicates that there exists one chemical state of Si in the silica films. It should be mentioned that the FWHM of Si 2p from a clean Si(111)-7×7 surface was measured at 1.4 eV. The FWHM of Si 2p from the silica films (2.3 eV) is around 1.6 times of that from Si 2p of Si(111)

Table 1
HREELS frequencies of Si–O–Si vibrational modes on different silica samples

	Si–O–Si bending	Si–O–Si symmetric stretching	Si–O–Si asymmetric stretching		Refs.
HREELS (cm^{-1})	498	798	1176	SiO_2(0001)	[28]
	486–400	819–775	1153–1085	95–2 nm SiO_2/Si(100)	[28]
	480	840	1180	0.5 nm SiO_2/Si(111)	[31]
	365–400	740–790	1095–1150	1.0–1.3 ML SiO_2/Si(100)	[28]
	464	824	1184	2 nm SiO_2/Si(111)	[24]
	–	–	1060–1120	1–3 ML SiO_2/Si(100)	[4]
	424	–	1120	2.7 ML SiO_2/Si(100)	[5]
	496	798	1176	5 ML SiO_2/Mo(112)	[14]
	–	–	1048 (Si–O–Mo)	1 ML SiO_2/Mo(112)	[14]
	458	819	1100	This work	–

surface, which was also reported in many previous works [21,22].

At thick silica films, e.g. 2.8 and 6.5 nm silica layers, the Si 2p spectra present a small shoulder peak at low binding energy, originating from silicon suboxide. Additionally, the ratio of Si to O in the as-grown silica films has been calculated to be 0.42 and 0.48 for 2.8 and 6.5 nm films respectively using XP Si 2p and O 1s peak areas (due to the overlapping between Pd 3p, 532.3 eV, and O 1s, 533 eV, the calculation is more accurate for thicker silica films). The result is consistent with the Si 2p binding energy data, suggesting that we have deposited stoichiometric silica films. The lower binding energy for the 0.4 nm SiO_2 film is probably caused by the interaction between the ultrathin oxide film and the metal substrate, for example, the final state relaxation effect due to the screening of excited hole states by the image potential in the metal substrate [23]. Since the Si(IV) (103.3 eV) and Si(III) (101.6 eV) [21] peaks are close to each other, the shift could also be caused by insufficient oxidation of Si with the presence of Pd. For example, Schleich et al. [24] examined the Si 2p XP spectra by depositing a Pd film on a thin silica film and found that the Si peak shifted to lower binding energy. They explained that this shift was due to the oxygen vacancies in SiO_2 film being occupied by the deposited Pd atoms. Komiyama and Shimaguchi [25] obtained the same results in Pt-, Pd-, Ag- and Au-SiO_2 systems.

We also notice that the Pd 3d peaks present very small binding energy shifts (~0.1 eV) for the Pd(100) surface covered by silica films. It indicates that no Pd-silicide is formed at the silica/Pd(100) interface, in contrast with the formation of Ni-silicide layer at the SiO_2/Ni(111) interface [15]. The difference may be due to the different preparation methods and oxygen pressures during the experiment processes.

The valence bands of the silica films with thickness of ~1.1 nm and ~2.8 nm were measured by UPS with the He I radiation, shown in Fig. 2. Two major peaks are observed in both spectra. The features at ~8 eV correspond to the two O 2p nonbonding states (not resolvable from our measurements) and that at ~11.8 eV to the Si–O bonding state [26,27]. The dip between bonding and nonbonding states (at about 10 eV) is an important feature indicating the degree of crystallization of SiO_2 [26,27]. At this position, there could be some mixed states from the local topological disorder, fluctuations, and bond dimerizations, which will result in a less pronounced dip in a disordered SiO_2 phase, such as amorphous SiO_2. Fig. 2 shows that the

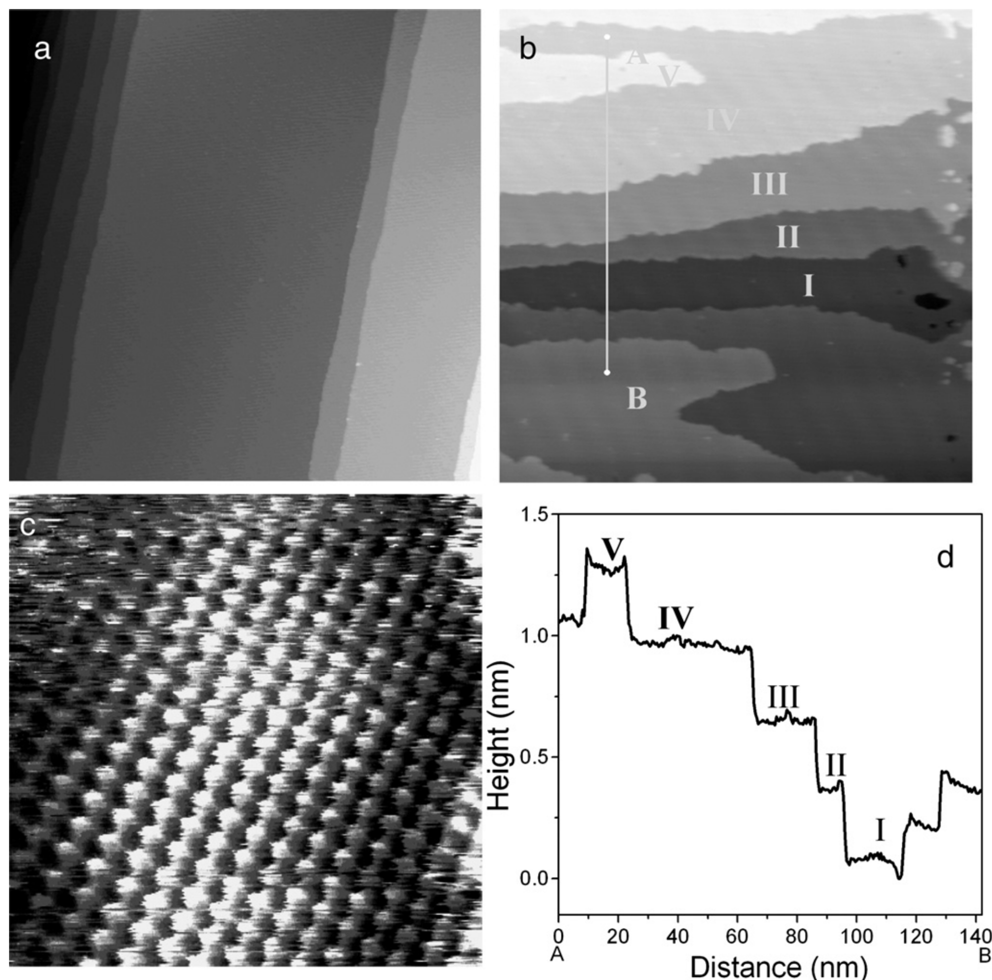

Fig. 4. STM images of (a) bare Pd(100) surface, 400 nm × 400 nm, Vs = 0.2 V, I = 0.47 nA (b) 2.8 nm thick silica film on Pd(100), 200 nm × 200 nm, Vs = 2.5 V, I = 0.18 nA (c) high resolution of (b), 5.6 nm × 5.6 nm, Vs = 2.0 V, I = 0.07 nA. (d) The height profile along the A–B line in (b). Layers have been indicated by Roman numerals in b and d.

spectra from 1.1 nm and 2.8 nm SiO_2 films have deep and sharp dips, implying that both films are highly ordered. This can be further proved by our STM measurements shown below.

Furthermore, the UPS results show that there is a notable difference between 2.8 nm and 1.1 nm silica film near E_F. One is that the whole spectrum shifts to higher binding energy with the increasing thickness, which may be due to the band bending of SiO_2 film near the metal-oxide interface. The other difference is that the feature near E_F originating from the metal support [26] could be seen from the 1.1 nm silica film rather than from the 2.8 nm film. The disappearance of such a feature near E_F (Fig. 2b) suggests that the 2.8 nm silica film must be thick enough (at least a few monolayer (ML)) such that the Pd signals can be totally attenuated. The UPS results indicate that our SiO_2 films have similar electronic band structure as that of the crystalline bulk SiO_2 [27].

HREELS has also been applied to characterize the 2.8 nm silica film, as shown in Fig. 3. Five inelastic scattering peaks were detected at 458, 827, 1106, 1541, and 2200 cm^{-1}, and the 1106 cm^{-1} phonon peak dominates the HREEL spectrum. The features at 458, 827 and 1106 cm^{-1} are assigned to the bending, symmetric stretching, and asymmetric stretching modes of Si–O–Si, respectively [14,28,29]. The peaks at 1541 and 2200 cm^{-1} correspond to combination band and overtone. For comparison, Table 1 lists the HREELS vibrational results from various amorphous and crystalline silica samples. It can be seen that it is not uncommon to see some differences in the frequencies reported by different groups. The HREELS experiment for crystalline SiO_2 is only reported by Thiry et al. [28]. The 1106 cm^{-1} loss in our work is lower than that of the SiO_2 (0001) [28]. Nevertheless, the value is still comparable to some other HREELS results (Table 1). The difference may be due to the different silica structures [5,30]. Nakagawa et al. [5] investigated the Si–O–Si structural changes by using a central-force-network model. They found that the vibrational frequencies varied with the structure relaxations via the force constants and bond angles of Si–O–Si. One may also suggest that there may exist some Si(II)–O species, which are the gas phase precursors of the SiO_2 film evaporated from the Si source in an oxygen background [9], responsible for the lower vibrational frequency. However, our XPS data (Fig. 1) demonstrate that the Si(IV) is the dominant species and the vibrational frequency of the Si–O molecule is 1230 cm^{-1} [31]. No Pd–O vibration peaks were observed indicating that no Pd diffused to the surface.

We used STM to investigate the morphology of the 2.8 nm thick silica film formed on the Pd(100) substrate, as displayed in Fig. 4 together with a bare Pd(100) image. It is shown from Fig. 4b that the SiO_2 film surface is very smooth and homogeneous, and the roughness in the terrace is far below one atomic layer (about 0.02 Å), and the terraces are notably free of voids and any other defects. The steps in the film show different orientation and shape as that of on the bare Pd(100) surface in Fig. 4a. The step height is measured to be 2.8±0.2 Å, 1.4 times of Pd(100) step height. Thus, we suggest that the observed steps in Fig. 4b should be from the silica film surface rather than those of Pd(100) surface. The height profile of A–B line across the steps (Fig. 4d) also indicates that the film has multilayer structure (layers have been indicated by Roman numerals in Fig. 4b). Fig. 4c gives the calibrated atomic resolution STM image of the SiO_2 film surface. Calibration of the image by Si(111)-7×7 allows measuring the lattice constant of the SiO_2 film at 3.6± 0.2 Å, which is close to the $\sqrt{2}$ times that of Pd(100). Some STM measurements of silica films formed on Mo(112) [13,32], Ni (111) [15], and Si(111) [3] surfaces had also been reported. Schroeder et al. and Min et al. studied the structure of 1 ML (~0.3 nm thick) silica films on Mo(112) with a well-ordered surface structure [10–13,32]. The unit cell spacing was determined to be about 5±0.5 Å by STM, which was in reasonable agreement with their low energy electron diffraction measurements. However, the thicker films in their papers all show poor long-range order. Our STM measurement shows that SiO_2 film prepared by our method is highly ordered in a long range, as also confirmed by the UPS and HREELS. The structure and the growth mechanism still need to be further investigated.

The thermal stability of the SiO_2 films was also investigated. Fig. 5 presents a set of ISS data recorded from a 2.8 nm silica films upon annealing at different temperatures. Fig. 5a is the ISS from the as-deposited silica film, showing two peaks with the kinetic energy at about 410 and 600 eV, corresponding to O and Si elements, respectively. No Pd peak is observed, indicating no diffusion of Pd to the surface at the silica growth temperature (500 K). After annealing at 800 K for longer time (13 min vs. 3 min, shown by Fig. 5b and c), a trace of Pd peak at 880 eV is detected. Correspondingly, our XPS experiments show a small increase in the Pd 3d peak intensity. However, no shift of the peak position is observed (not shown). ISS measurement on the 1050 K annealed film shows a much clearer Pd peak (see Fig. 5d), implying that Pd may diffuse in the silica film at 800 K with a slow rate compared with those reported on the SiO_2 films

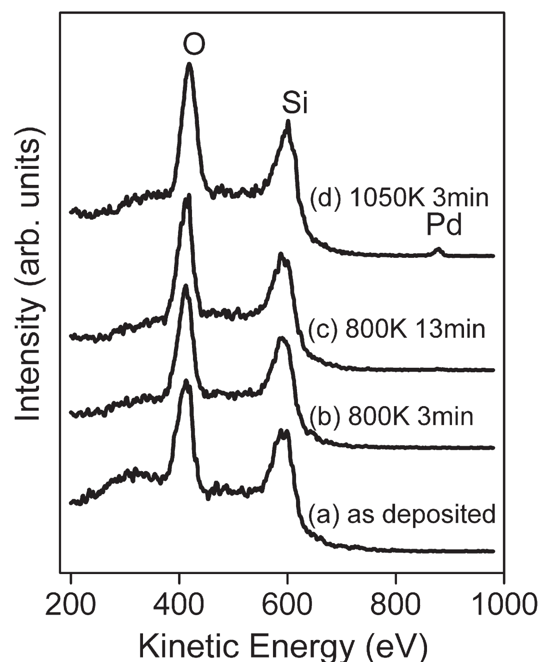

Fig. 5. The ISS spectra of silica films on Pd(100) after various thermal treatments (a) as deposited, (b) annealing at 800 K for 3 min, (c) annealing at 800 K for 13 min, (d) annealing at 1050 K for 3 min. The spectra were collected at RT.

formed on Mo substrate [33]. This may be due to the low defect density in our silica films. Min et al. have studied the thermal stability of Pd overlayers supported on single crystalline SiO_2 thin films grown on Mo(112) substrate. They found that Pd started to diffuse into SiO_2 when the substrate was heated to above 700 K and Pd silicide formation occurred between 850 and 1000 K on defective silica films [33].

4. Conclusions

We demonstrated a method of preparation of ultrathin silica films on a Pd(100) surface by depositing silicon in the 1×10^{-3} Pa oxygen pressure at 500 K. SiO_2 films with different thicknesses (0.4–6.5 nm) have been prepared. The 2.8 nm silica film shows smooth morphology, stoichiometry, and well-ordered structure in a long range. The lattice structure of the SiO_2 film is closely related with the Pd substrate structure, with a lattice constant of 3.6 ± 0.2 Å, similar to $\sqrt{2}$ times of the Pd(100) surface's lattice constant. The low density of defects in the films makes the films very stable, which prevents the diffusion of the supporting metal or the formation of silicide. The flat and ordered silica ultrathin films may be used as the model supports for growth of metal catalysts.

Acknowledgements

This work was financially supported by the National Natural Science Foundation of China (No. 90206036 and No. 20573107). We acknowledge Dr. Zhen Song, Prof. Qinlin Guo, and Dr. Xiulian Pan with pleasure for helpful discussions and critically reading the manuscript.

References

[1] J.B. Zhou, T. Gustafsson, E. Garfunkel, Surf. Sci. 372 (1997) 21.
[2] J.T. Mayer, R.F. Lin, E. Garfunkel, Surf. Sci. 265 (1992) 102.
[3] J. Wang, C.E.J. Mitchell, R.G. Egdell, J.S. Foord, Surf. Sci. 506 (2002) 66.
[4] H. Ikeda, Y. Nakagawa, K. Sato, M. Higashi, S. Zaima, Y. Yasuda, Thin Solid Films 343–344 (1999) 408.
[5] Y. Nakagawa, M. Higashi, H. Ikeda, S. Zaima, Y. Yasuda, Appl. Surf. Sci. 130–132 (1998) 192.
[6] X.P. Xu, S.M. Vesecky, D.W. Goodman, Science 258 (1992) 788.
[7] X. Xu, D.W. Goodman, Surf. Sci. 282 (1993) 323.
[8] X. Xu, D.W. Goodman, Appl. Phys. Lett. 61 (1992) 774.
[9] J.W. He, X. Xu, J.S. Corneille, D.W. Goodman, Surf. Sci. 279 (1992) 119.
[10] T. Schroeder, M. Adelt, B. Richter, M. Naschitzki, M. Bäumer, H.J. Freund, Surf. Rev. Lett. 7 (2000) 7.
[11] T. Schroeder, A. Hammoudeh, M. Pykavy, N. Magg, M. Adelt, M. Baumer, H.J. Freund, Solid State Electron. 45 (2001) 1471.
[12] T. Schroeder, J.B. Giorgi, M. Bäumer, H.J. Freund, Phys. Rev. B 66 (2002) 165422.
[13] J. Weissenrieder, S. Kaya, J.L. Lu, H.J. Gao, S. Shaikhutdinov, H.J. Freund, M. Sierka, T.K. Todorova, J. Sauer, Phys. Rev. Lett. 95 (2005) 076103.
[14] M.S. Chen, A.K. Santra, D.W. Goodman, Phys. Rev. B 69 (2004) 155404.
[15] M. Kundu, Y. Murata, Appl. Phys. Lett. 80 (2002) 1921.
[16] R.G. Musket, W. McLean, C.A. Colmenares, D.M. Makowiecki, W.J. Siekhaus, Appl. Surf. Sci. 10 (1982) 143.
[17] W. Huang, R. Zhai, X. Bao, Langmuir 17 (2001) 3629.
[18] J.F. Moulder, W.F. Stickle, P.E. Sobol, K.D. Bomben, Handbook of X-ray Photoelectron Spectroscopy, Perkin-Elmer, Waltham, U.S.A., 1992.
[19] J.C. Ashley, C.J. Tung, Surf. Interface Anal. 4 (1982) 52.
[20] M.H. Schaffner, F. Patthey, W.D. Schneider, Surf. Sci. 417 (1998) 159.
[21] F.J. Himpsel, F.R. McFeely, A. Taleb-Ibrahimi, J.A. Yarmoff, G. Hollinger, Phys. Rev. B 38 (1988) 6084.
[22] M.P. Seah, S.J. Spencer, Surf. Interface Anal. 35 (2003) 515.
[23] G. Kaindl, T.C. Chiang, D.E. Eastman, F.J. Himpsel, Phys. Rev. Lett. 45 (1980) 1808.
[24] B. Schleich, D. Schmeisser, W. Göpel, Surf. Sci. 191 (1987) 367.
[25] M. Komiyama, T. Shimaguchi, Surf. Interface Anal. 32 (2001) 189.
[26] Y.D. Kim, T. Wei, D.W. Goodman, Langmuir 19 (2003) 354.
[27] A. Di Pomponio, A. Continenza, L. Lozzi, M. Passacantando, S. Santucci, P. Picozzi, Solid State Commun. 95 (1995) 313.
[28] P.A. Thiry, M. Liehr, J.J. Pireaux, R. Sporken, R. Caudano, J.P. Vigneron, A.A. Lucas, J. Vac. Sci. Technol. B 3 (1985) 1118.
[29] J.A. Schaefer, W. Göpel, Surf. Sci. 155 (1985) 535.
[30] L. Giordano, D. Ricci, G. Pacchioni, P. Ugliengo, Surf. Sci. 584 (2005) 225.
[31] H. Ibach, H.D. Bruchmann, H. Wagner, Appl. Phys. A 29 (1982) 113.
[32] B.K. Min, W.T. Wallace, A.K. Santra, D.W. Goodman, J. Phys. Chem. B 108 (2004) 16339.
[33] B.K. Min, A.K. Santra, D.W. Goodman, Catal. Today 85 (2003) 113.